



HAL
open science

Optimization of Paracetamol and Chloramphenicol Removal by Novel Activated Carbon Derived from Sawdust Using Response Surface Methodology

Mohamed Romdhani, Afef Attia, Catherine Charcosset, Samia Mahouche-Chergui, Ayten Ates, Joelle Duplay, Raja Ben Amar

► **To cite this version:**

Mohamed Romdhani, Afef Attia, Catherine Charcosset, Samia Mahouche-Chergui, Ayten Ates, et al.. Optimization of Paracetamol and Chloramphenicol Removal by Novel Activated Carbon Derived from Sawdust Using Response Surface Methodology. *Sustainability*, 2023, 15 (3), pp.2516. 10.3390/su15032516 . hal-04073296

HAL Id: hal-04073296

<https://hal.science/hal-04073296>

Submitted on 18 Apr 2023

HAL is a multi-disciplinary open access archive for the deposit and dissemination of scientific research documents, whether they are published or not. The documents may come from teaching and research institutions in France or abroad, or from public or private research centers.

L'archive ouverte pluridisciplinaire **HAL**, est destinée au dépôt et à la diffusion de documents scientifiques de niveau recherche, publiés ou non, émanant des établissements d'enseignement et de recherche français ou étrangers, des laboratoires publics ou privés.

Article

Optimization of Paracetamol and Chloramphenicol Removal by Novel Activated Carbon Derived from Sawdust Using Response Surface Methodology

Mohamed Romdhani ^{1,2}, Afef Attia ¹, Catherine Charcosset ², Samia Mahouche-Chergui ³, Ayten Ates ⁴, Joelle Duplay ⁵ and Raja Ben Amar ^{1,*}

¹ Research Unit “Advanced Technologies for Environment and Smart Cities”, Faculty of Science of Sfax, University of Sfax, Sfax 3038, Tunisia

² LAGEP, UMR 5007, CNRS, Université Claude Bernard Lyon 1, 43 Boulevard du 11 Novembre 1918, F-69100 Villeurbanne, France

³ Institut de Chimie et des Matériaux Paris-Est (ICMPE), UMR 7182 CNRS, Université Paris-Est, 2 Rue Henri Dunant, F-94320 Thiais, France

⁴ Department of Chemical Engineering, Engineering Faculty, Cumhuriyet University, 58140 Sivas, Türkiye

⁵ EOST-LHYGES, UMR 7517, CNRS, Université de Strasbourg, F-67084 Strasbourg, France

* Correspondence: benamar.raja@yahoo.com

Abstract: Paracetamol (PCT) and chloramphenicol (CPL) can have unfavorable impacts on human health, as well as on natural ecosystems. These substances contribute to the aquatic environment’s contamination and disturb the performance of municipal wastewater treatment systems, causing ecosystem disruption and microbial resistance. In this study, activated carbon produced from sawdust (ACs) was synthesized utilizing the chemical activation process for the removal of both PCT and CPL compounds from an aqueous solution. ACs has a primarily microporous structure with a significant specific surface area of 303–1298 m²/g, total pore volume of 0.462 cm³/g and bimodal distribution of pores of 0.73–1.7 nm. The removal efficiencies for PCT and CPL with the low-cost activated carbon, determined at the optimum dose (750 mg/L for PCT and 450 mg/L for CPL), were significantly high at 85% and 98%, respectively. The adsorption kinetics for both pharmaceuticals exhibited a quick initial decline. For PCT and CPL adsorption, the equilibrium was attained after just 20 and 90 min, respectively. The Langmuir isotherm model and the pseudo-second-order kinetics model offered the best fits for the adsorption of both compounds. Additionally, the central composite design (CCD) and Box–Behnken design (BBD) were used to optimize the experimental adsorption conditions using a response surface methodology (RSM). On the basis of the findings, it is evident that activated carbon made from sawdust may be used as a new, effective alternative adsorbent for removing PCT and CPL in aqueous environments.

Keywords: paracetamol; chloramphenicol; activated carbon; adsorption; response surface; methodology; experimental design



Citation: Romdhani, M.; Attia, A.; Charcosset, C.; Mahouche-Chergui, S.; Ates, A.; Duplay, J.; Ben Amar, R. Optimization of Paracetamol and Chloramphenicol Removal by Novel Activated Carbon Derived from Sawdust Using Response Surface Methodology. *Sustainability* **2023**, *15*, 2516. <https://doi.org/10.3390/su15032516>

Academic Editors: Mikhael Bechelany and Jagpreet Singh

Received: 4 November 2022

Revised: 2 January 2023

Accepted: 4 January 2023

Published: 31 January 2023



Copyright: © 2023 by the authors. Licensee MDPI, Basel, Switzerland. This article is an open access article distributed under the terms and conditions of the Creative Commons Attribution (CC BY) license (<https://creativecommons.org/licenses/by/4.0/>).

1. Introduction

In recent years, global attention has been paid to environmental challenges, such as climate change, soil contamination and air and water pollution. As population health and water pollution concerns evolve, more work is needed to remove contaminants from water sources [1,2].

Pharmaceutical compounds are considered some of the most important emerging contaminants of water resources [3]. Various examples of such compounds have been detected in wastewater [4,5], and many studies have confirmed that these compounds can have unfavorable impacts on human health, as well as on natural ecosystems [3,6]. Among pharmaceuticals, antibiotics can be classified as a special class. They have received

particular interest because they are biologically active and, albeit at modest concentrations, induce bacterial resistance with constant exposure [7]. Antibiotic contamination has been shown to degrade water quality in river systems, irrigation canals, lakes and reservoirs in several studies [8]. One such antibiotic pollutant is chloramphenicol [9], which is a bacterial antibiotic with a broad range of activity. As a result, chloramphenicol pollutes aquatic resources, hospital effluents and sewage treatment facilities, causing ecosystem disruption and microbial resistance [10,11]. In addition, paracetamol (acetaminophen) is among the pharmaceutical compounds that are most frequently prescribed and used globally to treat fever, pain and inflammation for adults and children [12]. Due to its special physicochemical features and interaction model with aquatic species, PCT has been consistently described as the most important contaminant in the aquatic environment [13,14]. As a result, before discharging wastewater into the environment, it is critical to remove antibiotic substances through specific treatments.

In the literature [15], several technologies for wastewater treatment have been reported, such as adsorption, the membrane procedure, coagulation–flocculation and advanced oxidation methods. The adsorption process is of tremendous interest for water and wastewater treatment because of its removal effectiveness, ease of installation, operational simplicity and low cost [15,16]. In one study, different adsorbents [15] were used to eliminate several pharmaceutical substances from an aqueous medium. Due to its enormous surface area and high level of porosity, activated carbon was considered suitable for use in the treatment of wastewater and air pollution [17,18]. Lach et al. [19] investigated chloramphenicol removal using activated carbon with a high specific surface area and pore volume ($1692 \text{ m}^2/\text{g}$, $2.103 \text{ cm}^3/\text{g}$). They found a good adsorption capacity for chloramphenicol of $214 \text{ mg}/\text{g}$. Another group of researchers [20] are concentrating their efforts on producing low-cost activated carbon based on natural and widely available materials, such as biomass, agricultural wastes and effluent sludge. Streit et al. [21] used two types of activated carbon prepared from effluent treatment plant sludge (BSAC and ABSAC) to investigate its performance in eliminating three pharmaceutical substances (ibuprofen, ketoprofen and paracetamol). For ibuprofen, ketoprofen and paracetamol, the highest adsorption capacities with the ABSAC were found to be equal to 105, 57 and $145 \text{ mg}/\text{g}$, respectively. Furthermore, the existence and availability of raw carbon materials, as well as the seasonal variations in the raw material quality, should be taken into account when producing activated carbon. Additionally, the activation procedures and chemical activators selected are very important for the production of activated carbon with good quality and higher efficiency for the elimination of various contaminants. Activated carbon can be produced in two ways depending on the nature of the activation procedure: chemically or physically [22]. In physical activation [22,23], the raw materials start by undergoing a pyrolysis step (carbonization) in a neutral atmosphere and, after that, the process continues with activation in atmospheric oxidizing gases, such as carbon dioxide, a mixture of carbon dioxide and nitrogen or a blend of air and steam, in the temperature range from 800 to $1100 \text{ }^\circ\text{C}$. Yahya et al. [24] found that this method is environmentally friendly because it is chemical-free, and it can generate activated carbon with a porous structure and good physical performance. However, the fundamental drawbacks of this method are that the resultant activated carbon has a limited adsorption capacity and extensive activation time and its production involves significant energy consumption. In the chemical activation method [22], the raw materials are reacted with chemical activators at temperatures ranging between 400 and $900 \text{ }^\circ\text{C}$. Many chemical activators are used, such as zinc chloride, potassium hydroxide, potassium carbonate, sodium hydroxide and phosphoric acid. The nature of the chemical activators plays an important role on the amount and quality of activated carbon produced. Yorgun et al. [25] used H_3PO_4 as a chemical activator to produce activated carbon from wood. They found that the phosphoric acid functioned as a moderator that enhanced porosity while also permitting the growth of acidic surface functional groups. They confirmed that carbon produced from H_3PO_4 activation had a larger surface area and total pore volume than carbon activated with ZnCl_2 and KOH . For batch-mode adsorption, the approach of

changing just one parameter at a time is the general strategy used to examine the factors impacting the adsorption process. This traditional technique can only be used if each factor has an influence on its own, and it does not explain how different parameters might increase or neutralize each other [20]. To achieve this, experimental conditions must be optimized, which not only saves materials and time but also helps determine the optimal increase in the adsorption performance. Recently, the response surface methodology (RSM) [26] has received a great deal of interest, not only because it reduces the number of trials required and allows researchers to analyze all elements at once but also because it allows researchers to investigate the interactions between variables. The central composite design (CCD) is one of the most famous RSM designs. With this design, all of the quadratic regression model's coefficients, as well as the relationships between various components, are taken into account. As a result, the best values for each variable, as well as their relative importance, can be easily determined [27,28]. The Box–Behnken design (BBD)-based RSM is commonly employed due to its appealing benefits, including the reduced number of trials required in comparison to other models, such as the Doehlert design or full-factorial design [29].

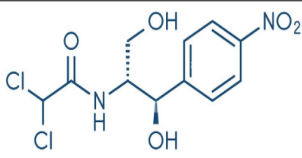
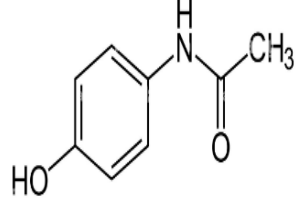
In the present study, sawdust was chosen as the raw material to synthesize activated carbon due to its availability and abundance. The chemical activation procedure was applied to produce the activated carbon. The objective was to characterize and study the effects of the experimental conditions on paracetamol (PCT) and chloramphenicol (CPL) removal from an aqueous medium. Thus, the central composite design (CCD) and the Box–Behnken design (BBD) were implemented to optimize the experimental adsorption settings using a response surface methodology (RSM) model.

2. Materials and Methods

2.1. Materials and Chemicals

The sawdust was collected from a wood factory that generated sawdust as trash. The pharmaceutical compounds studied were paracetamol (acetaminophen, >99%) and chloramphenicol (>98%). Both drugs (activated substances) were provided by Sigma-Aldrich. Phosphoric acid (H_3PO_4 , 85%) was utilized as a chemical activator. NaOH (0.2M) and HCl (0.2M) were employed to alter the pH. The principal characteristics of the chloramphenicol and paracetamol are shown in Table 1.

Table 1. Various characteristics of the drugs used.

Pharmaceutical Substance	Chemical Formula	Molecular Weight (g/mol)	λ_{max} (nm)	pKa	Water Solubility at 25 °C (g/L)	Structural Formula
Chloramphenicol (CPL)	$C_{11}H_{12}Cl_2N_2O_5$	323.13	279	5.52	2.5	
Paracetamol (PCT)	$C_8H_9NO_2$	151.16	245	9.38	13.85	

2.2. Activated Carbon Preparation

The origin of the raw material for the activated carbon was sawdust collected from a wood factory in the form of particles with an average size of less than 1 mm. Activated carbon was synthesized using a previously described protocol [30,31] with some modifica-

tions. Briefly, the raw sawdust was washed with distilled water and dried at 105 °C for 6 h. Then, an 85% concentrated solution of phosphoric acid was used to soak the pretreated sawdust at a weight ratio of 1/4. After 30 h, the sawdust–H₃PO₄ was dried for 12 h at 105 °C and then carbonized at 700 °C for 1.2 h in N₂ media with a heating rate of 5 °C/min. The treated sawdust was washed with diluted NaOH to eliminate excess phosphoric acid and then with distilled water many times. Finally, the resulting activated carbon based on sawdust (ACs) was gently ground and passed through a 100 µm mesh.

2.3. Characterization

The samples were characterized using Fourier-transform infrared spectroscopy (FTIR) with a Bruker TENSOR 27 (Bruker Optics Ltd., Coventry, UK) to investigate the functional groups on their surfaces. Measurements of the X-ray diffraction of the AC₅ were performed with a powder diffractometer (Bruker D8 Advance diffractometer) using Cu-K α radiation ($\lambda = 1.54 \text{ \AA}$) scanning from 4° to 80° in 2 θ scans. Thermogravimetric analysis (TGA) was carried out with a ACs size below 100 µm and mass of 20 mg. The tests were carried out using a thermogravimetric analyzer (SetaramSetsys Evolution 16 apparatus) at a heating rate of 10 °C/min under an argon atmosphere, and the ACs was heated from 20 to 1000 °C. Scanning electron microscopy (SEM, Zeiss MERLIN) was also carried out to investigate the morphologies of the samples. An ASAP 2020 instrument (Micromeritics, France, S.A.R.L) and the Brunauer–Emmett–Teller (BET) method were used to determine the total pore volume, pore diameter and the specific surface area, while a zetameter (Zeta Sizer Nano series 25) was used to determine the point of zero charge (pHpzc). In order to determine the interactions with the ACs, the adsorption efficiency of the PCT and CPL onto ACs was examined using a UV–Vis spectrophotometer (UV 7205 JENWAY spectrophotometer). The pharmaceutical molecule concentrations were analyzed at a wavelength of 245 nm for PCT and 279 nm for CPL. The pH values were determined using a pH meter (SevenCompact pH meter S220).

2.4. Adsorption Experiments

ACs adsorbents were applied for PCT and CPL adsorption. To achieve this, 100 mg/L PCT and CPL standard solutions were produced weekly in distilled water. The standard solutions were diluted with distilled water and used in the experiments at the necessary concentrations. The tests were carried out by adding a certain amount of ACs to 100 mL of the pharmaceutical solution (PCT or CPL) agitated at 450 rpm using a magnetic stirrer (WiseStir HS-100D, Witeg). Various conditions were used in the experiments, including variations in the adsorbent dosage, contact time, pH, pharmaceutical solution initial concentration and temperature. The adsorbent dose was varied from 100 mg/L to 900 mg/L and the contact time from 5 min to 150 min, and the pH values were altered within the range from 2.5 to 12.5 using HCl (37%) and NaOH (0.2M) solutions. PCT and CPL initial concentrations were varied from 10 mg/L to 100mg/L. Finally, the temperature was adjusted within the range from 293 to 313 K to investigate its effect on the adsorption process. Following each test, the ACs adsorbent was separated from the PCT and CPL solutions using a 0.45 µm syringe filter. The residual PCT and CPL concentrations were measured using a UV–visible spectrophotometer at wavelengths of 245 nm for PCT and 279 nm for CPL. The pharmaceutical removal efficiency was determined using Equation (1):

$$R(\%) = \frac{(C_i - C_e)}{C_i} \times 100 \quad (1)$$

The adsorption capacity for the pharmaceutical compounds by ACs was determined with Equation (2):

$$qe = \frac{(C_i - C_e)}{m} \times V \quad (2)$$

where C_i and C_e are the initial and equilibrium pharmaceutical concentrations (mg/L), V is the volume of the pharmaceutical solution (L) and m is the weight of the adsorbent (g).

2.5. Experimental Design

Even in the presence of complicated interactions, the RSM can be used for the determination and assessment of the relative relevance of parameters through a mix of mathematical and statistical approaches followed by optimum region determination. Modeling is undertaken by adapting first- or second-order polynomial equations to the experimental responses collected through the experimental design and then analyzing the model using a variance analysis (ANOVA) [32] to identify the variables' substantial impacts and determine the model robustness. The verified model can be displayed as a 3D graph to provide a surface response that correlates with a response function, which is used to find the ideal operating parameters for a process (here using Expert Design V12). It is important to analyze and determine the most significant variables using an appropriate model with a limited number of runs. Thus, a response surface methodology (RSM) based on the central composite design (CCD) [29] was used to modulate the experimental conditions of the process of the adsorption of chloramphenicol by the activated carbon. The variables studied were adsorbent dosage (A_1) and chloramphenicol concentration (A_2). The total number of experiments required (N_C) was calculated using Equation (3):

$$N_C = 2^k + 2k + C_0 \quad (3)$$

where k is the number of factors, 2^k represents the cubic runs, $2k$ represents the axial runs and C_0 is the number of repeats in the center point's runs.

Table 2 presents independent factors and their low (−1), central (0) and high (1) levels, which correspond to the lowest, middle, and highest values, respectively.

Table 2. Experimental factors and levels in the CCD.

	Factor Levels		
	Low (−1)	Central (0)	High (1)
(A_1) Adsorbent Dosage (mg/L)	100	450	800
(A_2) CPL Concentration (mg/L)	10	55	100
Runs	A_1	A_2	Removal (%)
1	800	100	98
2	450	100	63
3	800	10	98
4	450	55	93
5	100	100	2.6
6	450	55	89
7	450	10	96
8	100	55	26
9	800	55	99
10	450	55	93
11	100	10	82.3

The CCD model is described by Equation (4):

$$Y(\%) = b_0 + \sum b_i A_i + \sum \sum b_{ij} A_i A_j + \sum \sum b_{ii} A_i^2; \quad i \neq j \quad (4)$$

where Y is the predicted response (removal percentage) and A_i represents the independent variables (CPL concentration and adsorbent dosage). The parameter b_0 is the model constant, b_i is the linear coefficient, b_{ii} represents the quadratic coefficients and b_{ij} represents the cross-product coefficients.

A RSM based on the Box–Behnken design (BBD) [29] was used to modulate the experimental conditions of the process of adsorption of paracetamol by the activated carbon. The variables studied were adsorbent dosage (X_1), pH (X_2) and paracetamol

concentration (X_3). The total number of experiments required (N_B) was calculated using Equation (5):

$$N_B = 2k(k - 1) + C_0 \quad (5)$$

where k is the number of variables and C_0 is the number of center point repeats.

The BBD model is described by Equation (6):

$$Y(\%) = b_0 + \sum b_i X_i + \sum \sum b_{ij} X_i X_j + \sum \sum b_{ii} X_i^2; i \neq j \quad (6)$$

where Y is the predicted response (removal percentage) and X_i represents the independent variables (PCT concentration, pH and adsorbent dosage). The parameter b_0 is the model constant, b_i is the linear coefficient, b_{ii} represents the quadratic coefficients and b_{ij} represents the cross-product coefficients.

Table 3 presents the independent factors and their low (−1), central (0) and high (1) levels, which correspond to the lowest, middle, and highest values, respectively, for the BBD.

Table 3. Experimental factors and levels in the BBD.

		Factor Levels			
		Low (−1)	Central (0)	High (1)	
(X₁) Adsorbent Dosage (mg/L)		100	500	900	
(X₃) pH		2.5	7.5	12.5	
(X₃) PCT Concentration (mg/L)		10	55	100	
Runs	X ₁	X ₂	X ₃	Removal (%)	
1	900	2.5	55	95	
2	100	12.5	55	6.4	
3	100	2.5	55	17.5	
4	500	12.5	100	38.1	
5	500	12.5	10	21.8	
6	500	12.5	100	49.5	
7	500	7.5	55	65.0	
8	500	7.5	55	63.7	
9	900	12.5	55	30.8	
10	100	7.5	10	55.0	
11	500	7.5	55	67.0	
12	900	7.5	100	73.5	
13	900	7.5	10	95.0	
14	100	7.5	100	7.9	
15	500	2.5	10	87.3	

3. Results and Discussion

3.1. Characterization of ACs Adsorbent

The XRD pattern of the ACs is depicted in Figure 1a. The two large and wide peaks located at approximately 24° and 43° reveal the amorphous nature of the prepared activated carbon [33,34]. The thermal behavior of the ACs sample was analyzed and is shown in Figure 1b. It can be observed that the TG curve contains two phases, and based on the ACs DTG, 14% of the mass loss in the first phase (33 °C to 470 °C) could be ascribed to water loss from the evacuation of moisture and water in the interstitials of the ACs [21,35]. For the second phase (470 °C to 997 °C), there was a 55% decrease in mass due to the carbonaceous matrix decomposing and the carbonaceous skeleton partially decomposing [21]. From 33 to 997 °C, the residual mass was determined to be 31%.

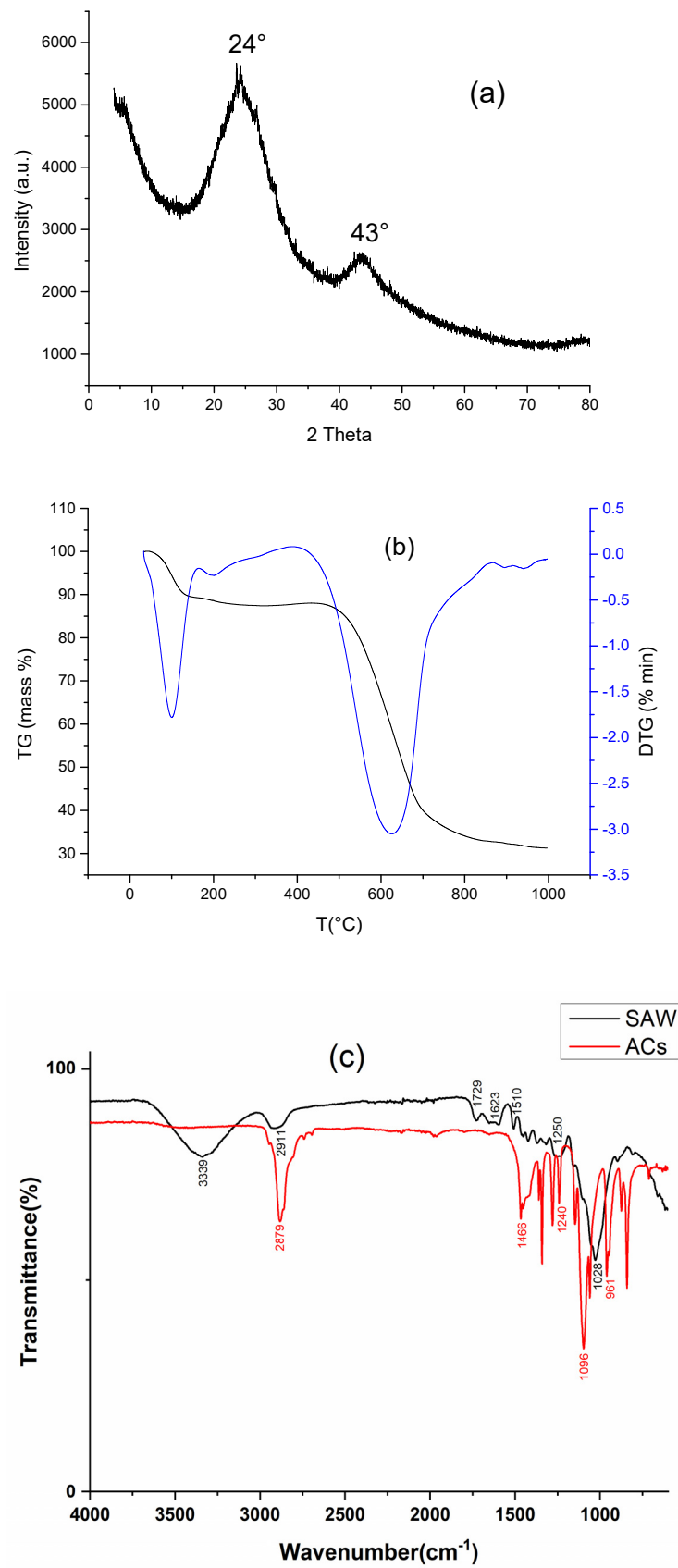


Figure 1. Cont.

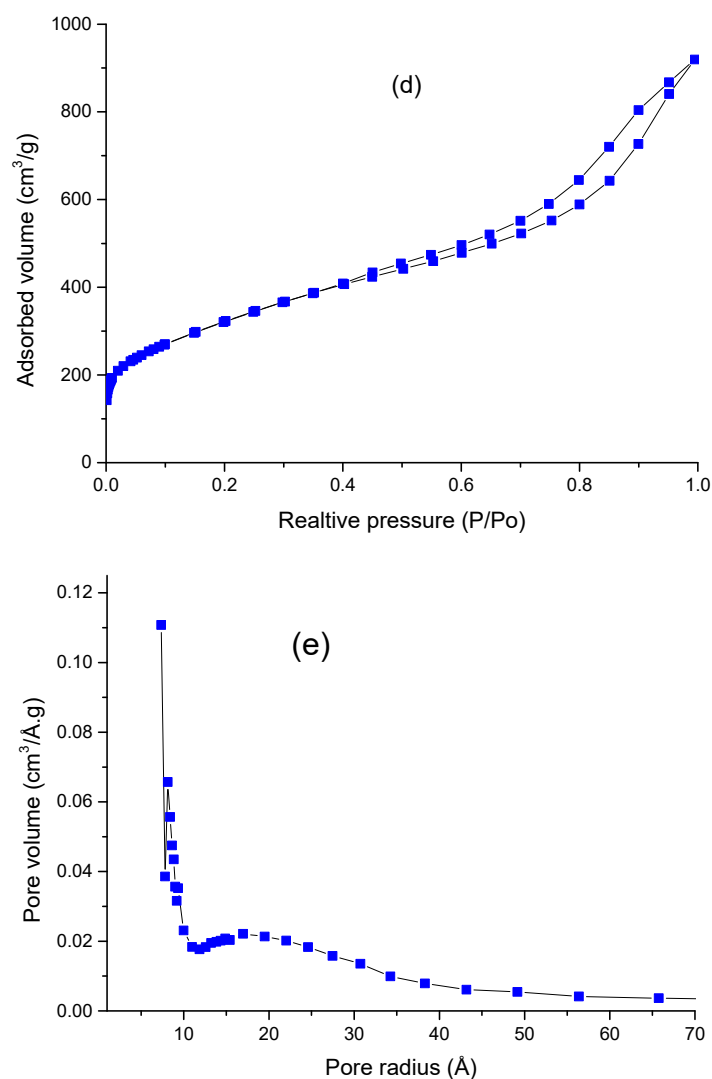


Figure 1. (a) XRD spectrum; (b) TG and DTG curves of ACs; (c) FTIR spectra for sawdust and ACs samples; (d) N_2 adsorption/desorption isotherms; (e) pore size distribution for ACs sample.

The FTIR spectra of sawdust and ACs were used to determine the functional groups. As can be clearly seen in Figure 1c, significant chemical changes were caused by the H_3PO_4 activation. The band situated at 3339 cm^{-1} (present only in the raw material) was essentially credited to the vibration stretching of O-H in phenol and hydroxyl bunches, a distinctive component of lignin [36]. The band situated at 2879 cm^{-1} was present in both samples, but with high intensity in the ACs. It was attributed to C-H stretching of methylene and methyl groups [37]. The peaks situated at 1623 and 1729 cm^{-1} related to C=C and C=O groups disappeared in the ACs FTIR [38]. The elimination of the groups of carbonyl may have been largely induced by the hydrolysis effect of H_3PO_4 . The peaks between 1510 and 1250 cm^{-1} were ascribed to C-H and O-H, respectively [39]. They were found in both samples, but with high intensity for ACs, which can be explained by the oxygenated functions generated by H_3PO_4 [40]. These observations show that there were significant implications of the chemical activation of the carbonaceous materials with phosphoric acid for the adsorption performance. While the peak situated at 1096 cm^{-1} was related to asymmetric vibration stretching of O-P-O [40], the peak that was altered from 1028 cm^{-1} in sawdust to 961 cm^{-1} in the ACs corresponded to a change from C-O, C=C and C-C-O stretching in the sawdust sample to P-O stretching in the ACs [40].

The results of the identification of the pore characteristics of the ACs sample are presented in Figure 1d,e, respectively. The material mostly had a mesoporous structure

according to IUPAC definitions (Figure 1d; type IV isotherm) [41,42], with a significant surface area and pore volume at 303–1298 m²/g and 0.462 cm³/g, respectively. The structure of microporous carbon was confirmed by a clearly bimodal distribution of pores of 0.73 and 1.7 nm (pore dimensions below 2 nm) [41]. Taking into account that the molecule sizes of pharmaceutical substances (paracetamol, chloramphenicol, ketoprofen, etc.) are in the order of magnitude of angstroms, it seems that the average pore size of the ACs was adequate to allow internal mass transfer of these substances into the adsorbent [43,44].

3.2. Adsorption Study of Paracetamol and Chloramphenicol

3.2.1. Effects of the Amount of Adsorbent

The adsorbent dosage used is widely recognized to have a significant influence on removal efficiency. A lower adsorbent dosage would provide greater benefits, such as savings in material and cost-effectiveness. Thus, the determination of the optimal amount of ACs showing maximum adsorption is a significant matter. Therefore, the effect of the adsorbent amount on both pharmaceutical compounds (PCT and CPL) was studied, as shown in Figure 2. It was found that increasing the ACs dosage led to the enhancement of the percentage of removal for each pharmaceutical. The removal efficiencies for PCT and CPL increased from 17% (at 100 mg/L) to 85% (at 750 mg/L) and from 37% (at 100 mg/L) to 98% (at 450 mg/L), respectively. This may be explained by the addition of more adsorbent to the solution, which increased the number of available adsorption sites and improved the ACs–PCT and ACs–CPL interaction probabilities, resulting in an increase in the removal efficiency, as already reported by other researches [16,21]. The equilibrium adsorption capacities (q_e) were determined for the two ACs dosages of 450 mg/L (CPL) and 750 mg/L (PCT) and found to be 88 mg/g and 45 mg/g, respectively. Beyond these ACs dosage values, the removal percentage was almost unaffected. This behavior may be explained by the agglomeration of the ACs particles [45]. Thus, the experimental results demonstrated that the optimal ACs dosages were 750 mg/L and 450 mg/L for PCT and CPL, and these values were applied in the following experiments. Previously, Cheng et al. [46] investigated the adsorption of chloramphenicol by corn stover-based activated carbon. They found that increasing the dosage of activated carbon from 2 to 20 g/L led to the enhancement of the chloramphenicol removal effectiveness from 90% to 100%, and they confirmed that 8 g/L was the optimal dosage.

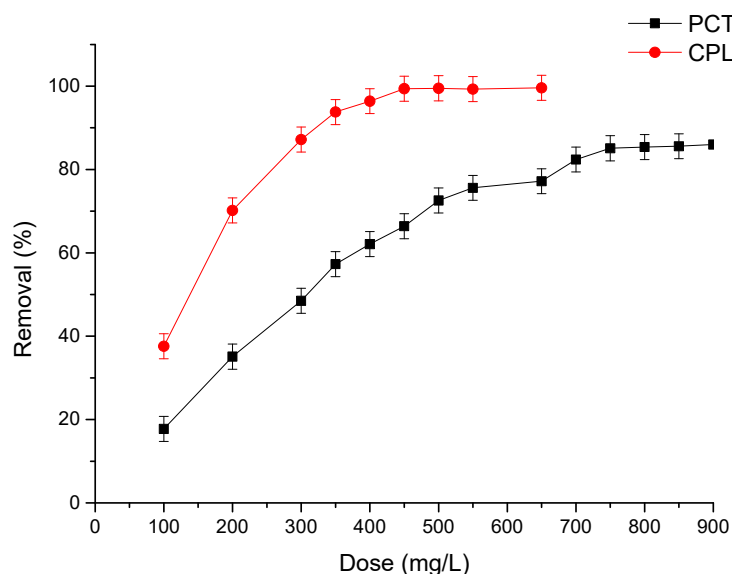


Figure 2. Effects of adsorbent dosages of ACs on PCT and CPL removal. $C_i = 40$ mg/L for PCT and CPL; $T = 25$ °C; $pH = 7.5$; $t = 150$ min.

3.2.2. Contact Time Effect

Contact time between the adsorbent and the adsorbed compound is a critical parameter since it strongly affects the adsorption efficiency. This parameter is very important in the design of an adsorption process and also determines the equilibrium time and the rate of adsorption [47]. In addition, this parameter plays a great role in energy saving and reductions of process costs. Therefore, the removal percentage for PCT and CPL was studied between 5 and 150 min, as shown in Figure 3. The adsorption of both pharmaceuticals increased quickly at the beginning of the process. After just 10 min, the ACs removed more than 80% of the PCT and more than 90% of the CPL. The adsorption rate significantly dropped after this period, and equilibrium was attained after 20 min (85%) and 90 min (98%) for PCT and CPL. The quick diffusion of CPL and PCT into the ACs' micropores during the first stage might explain this outcome. The adsorption sites on the surface of the ACs were then gradually occupied until equilibrium was attained [21,48]. Zhu et al. [49] reported comparable behavior in the adsorption rates across activated carbon matrices based on many precursors, such as chicken feathers, petroleum cokes, fallen leaves and *Enteromorpha prolifera*. They revealed that chloramphenicol adsorption by the different adsorbents was particularly fast during the first 5 min period and gradually increased thereafter. Indeed, Nourmoradi et al. [45] described the same behavior for the paracetamol and ibuprofen adsorption rate with acorn-based activated carbon. They found that the rate of the adsorption was very rapid at the start of the procedure (during the first 30 min) and then significantly dropped after this period, and the optimum adsorption was attained at just 120 and 150 min for ibuprofen and paracetamol, respectively.

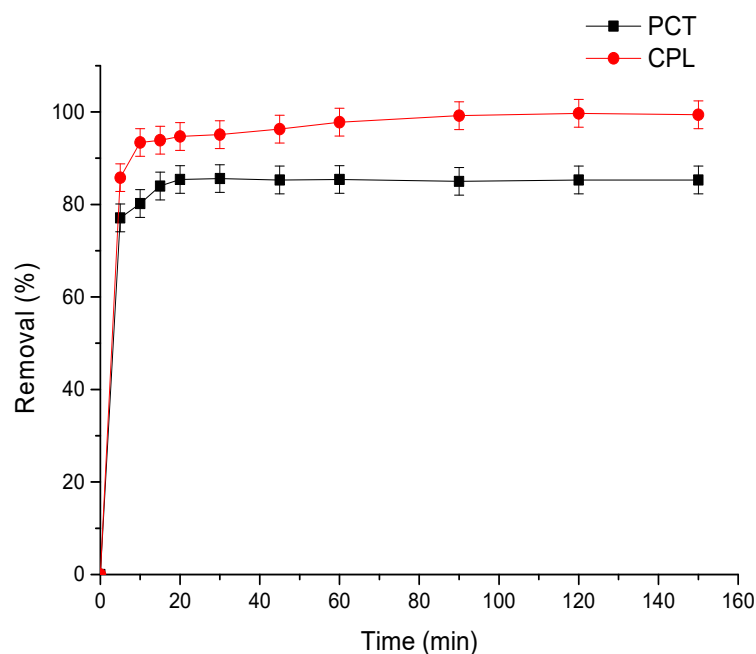


Figure 3. Effects of contact time on PCT and CPL removal. $C_i = 40$ mg/L for PCT and CPL; $T = 25$ °C; $pH = 7.5$; ACs dosage = 750 mg/L for PCT and 450 mg/L for CPL.

These findings indicate that the activated carbon produced from sawdust had a very high rate of adsorption for the removing of both pharmaceuticals.

3.2.3. Effect of pH Solution

The most significant factor influencing adsorption mechanisms is the pH solution level. This factor may be related to the physicochemical characteristics and the ionization of the adsorbate. The study of this factor was necessary for the investigation of the ACs–PCT and ACs–CPL interactions. The PCT and CPL removal percentages were investigated in the pH range between 2.5 and 12.5, as shown in Figure 4b. CPL removal was reduced

negligibly from 99.8% (pH of 2.5) to 93% (pH of 12.5). Furthermore, it was found that the removal of PCT changed from 89.5% to 84% when the pH changed from 2.5 to 9.4. However, it strongly decreased from 84% to 31.5% when the solution pH changed from 9.4 to 12.5. PCT and CPL are in their protonated forms (non-ionized) when the solution's pH is below pK_a [45]. The pK_a values for CPL and PCT were 5.52 and 9.38, respectively, as illustrated in Table 1. Therefore, both substances were charged negatively when the pH of the solution was superior to pK_a . With the protonation form of CPL ($pH < 5.52$), some functional groups of CPL, such as $-OH$ and $-NH-$, interact with oxygen on the surface of ACs [50]. The CPL molecule formed a hydrogen bond with ACs pores [48]. However, the deprotonated form of CPL occurred when the solution's pH value exceeded pK_a ($pH > 5.52$). As a result, the CPL-derived anions were repulsed from the negative surface of the ACs (Figure 4a) [51]. In the case of the PCT removal, the same behavior was seen. In the solution pH range below 9.38, the PCT molecules interacted with the surface of the ACs through hydrogen bonding interactions between the $-OH$ and $-NH$ groups in the PCT [52]. In the solution pH range up to 9.38, the PCT was in the ionized form (negative form). The strong reduction in the PCT removal rate can be explained by the electrostatic repulsion between the negative surface of the ACs and the anions of the PCT [53].

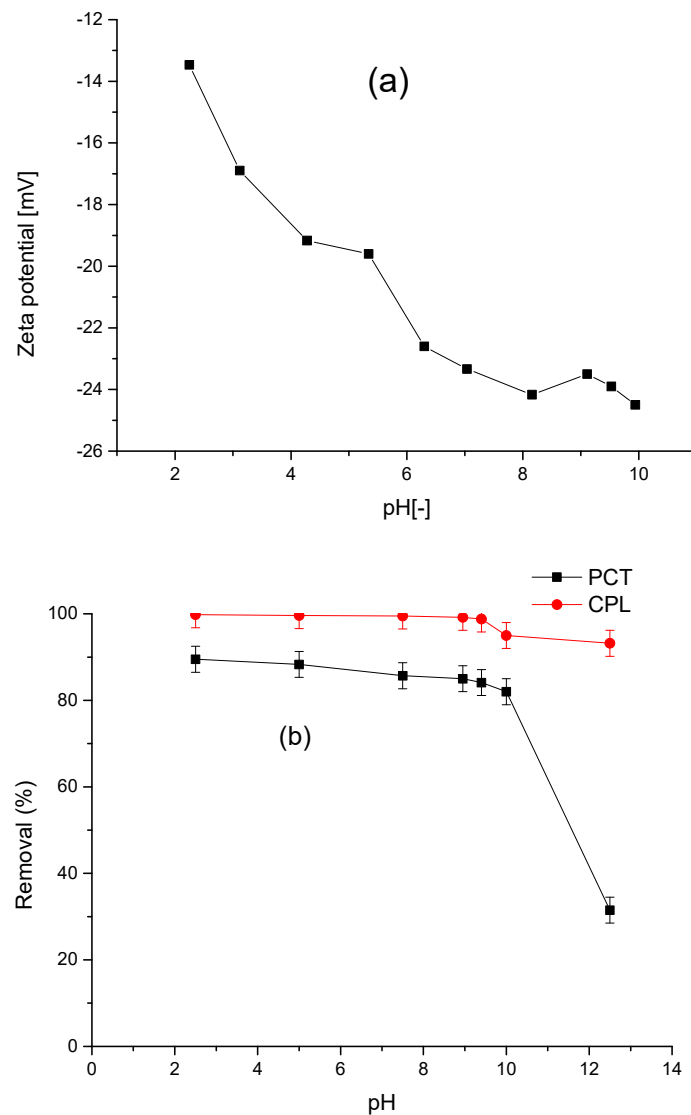


Figure 4. (a) Zeta potential of ACs; (b) effect of pH. $T = 25\text{ }^{\circ}\text{C}$; ACs dosage = 450 mg/L for CPL and 750 mg/L for PCT; $t = 90$ min for CPL and 20 min for PCT.

3.2.4. Effects of Initial Concentrations of PCT and CPL

Generally, the initial concentration is considered an important factor in adsorption procedures, especially for the determination of the adsorption capacity [54]. The effect of the initial concentration of PCT and CPL (10–100 mg/L) on the effectiveness of the adsorption of the ACs was investigated, and both removal percentages and adsorption capacities were determined (Figure 5a,b). As can be seen, the PCT and CPL removal rates decreased for initial concentrations between 10–100 mg/L from 89 to 64% and from 100 to 77.5%, respectively. This decrease could be understood in terms of the ratio of the active sites in the ACs and the pharmaceutical molecules, which is crucial at low concentrations to allow the uptake of all substances [16]. In contrast to the removal percentages, the adsorption capacity increased with greater PCT and CPL initial concentrations in the medium. It increased strongly from 11 to 92 mg/g for PCT and from 22 to 172 mg/g for CPL. This was in line with the change in the gradient of concentration, where PCT and CPL molecules showed a constant tendency to diffuse from the region of higher concentration (solution) to the region of lower concentration (adsorbent ACs) until equilibrium was reached in the system [55]. Zhao et al. [51] indicated that higher concentrations of CPL generated a greater number of functional groupings, including C=O, –NO₂ and –OH, resulting in increased interaction with the adsorbent's active sites and, thus, enhancing adsorption capacity. Nourmoradi et al. [45] found similar behavior for the adsorption of paracetamol and ibuprofen. They explained this effect in terms of the acceleration of driving forces, such as the van der Waals force, which takes precedence in the resistance against the transfer of the mass of a drug to the active sites of an adsorbent. This study demonstrated that the prepared sawdust-based activated carbon could be employed efficiently for PCT and CPL removal. In addition, the PCT and CPL contents in this range were substantially higher compared to the quantity of practical wastewater. In general, pharmaceutical compounds are present in municipal wastewater at very low concentrations in the order of ng/L and µg/L [15,56]. Therefore, the ACs developed in this work might be used in real applications.

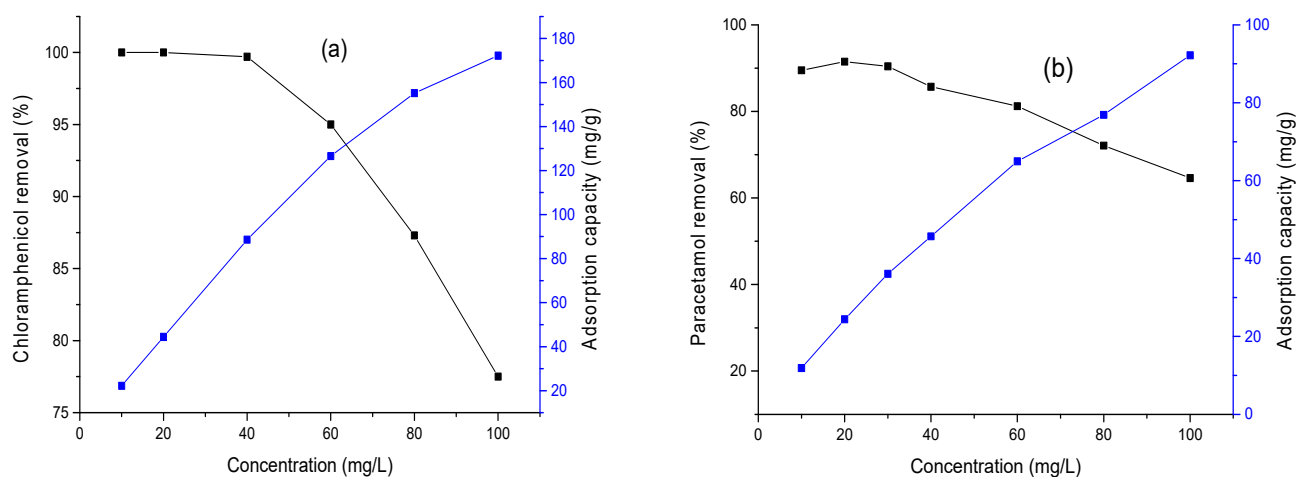


Figure 5. Effects of initial concentrations of (a) CPL (T = 25 °C; pH = 7.5; ACs dosage = 450 mg/L; t = 90 min) and (b) PCT (T = 25 °C; pH = 7.5; ACs dosage = 750 mg/L; t = 20 min).

3.2.5. Adsorption Kinetics

Kinetics investigations are critical for study of adsorption processes because they contribute to evaluating the rate and the mechanism of adsorption. The most frequent kinetic models used are pseudo-first-order (PFO) and pseudo-second-order (PSO) models [57]. The pseudo-first-order kinetic model is given as follows (Equation (7)):

$$\ln(q_e - q_t) = \ln q_e - K_1 t \quad (7)$$

where q_t and q_e are the quantities of PCT or CPL molecules adsorbed at t (min) and equilibrium (mg/g), respectively, and K_1 is the rate constant (min^{-1}). K_1 can be determined from the curve $\ln(q_e - q_t)$ vs. t .

The pseudo-second-order kinetic model is determined using Equation (8):

$$\frac{t}{q_t} = \frac{1}{(K_2 q_e^2)} + \frac{t}{q_e} \quad (8)$$

where K_2 (g/mg min) is the rate constant of adsorption and q_e is the equilibrium adsorption capacity (mg/g). The parameters are determined using the plot of t/q_t vs. t .

It is clear from Table 4 that the PSO kinetics correlated well with the uptake of PCT and CPL by the ACs. This model has an ideal fit for the results of the experiment, with correlation coefficients (R^2) very close to unity ($R^2 = 0.99$) for both pharmaceutical compounds. In addition, the equilibrium adsorption capacities calculated by the PSO model for PCT and CPL were close to those achieved experimentally. ACs showed various mechanisms for the adsorption of PCT and CPL, including adsorption onto the surface and diffusion into the ACs pores. PCT and CPL molecules began to enter the ACs pores and were adsorbed into the inner surface when active sites on the ACs surface reached saturation [58]. The k_2 value demonstrated that the diffusion of PCT molecules through the pores of the ACs was very rapid compared to the diffusion of CPL molecules (0.66 and 0.026 g/mg min for PCT and CPL, respectively). This explains why the PCT adsorption equilibrium was attained before that of CPL.

Table 4. Kinetic parameters for the PFO and PSO models.

	Pseudo-First-Order			Pseudo-Second-Order		
	k_1 (min^{-1})	q_e (mg/g)	R^2	k_2 (g/mg min)	q_e (mg/g)	R^2
PCT	0.2	49.38	0.81	0.66	50	0.99
CPL	0.047	111.7	0.93	0.026	85.7	0.99

3.2.6. Adsorption Isotherms

The determination of the isotherms of the adsorption process was very important for the identification of the interaction between the PCT and CPL molecules and the ACs. Various models have been used in the literature [57], such as the Langmuir [59] and Freundlich [60] models. The main hypothesis of the Langmuir isotherm model assumes monolayer adsorption on a homogeneous adsorbent surface and a lack of interaction between the adsorbate molecules on the surface of the adsorbent. Equations (9) and (10) present the Langmuir isotherm and the separation factor, respectively:

$$\frac{C_e}{q_e} = \frac{C_e}{q_m} + \frac{1}{q_m K_L} \quad (9)$$

$$\text{and } R_L = \frac{1}{(1 + K_L C_0)} \quad (10)$$

The Freundlich model is based on multilayer uptake onto the heterogeneous adsorbent surface. Equation (11) defines the Freundlich isotherm model:

$$\ln q_e = \ln K_f + \frac{\ln C_e}{n} \quad (11)$$

where C_e (mg/L) and q_e are, respectively, the concentration of PCT or CPL and the adsorption capacity (mg/g) of the ACs at equilibrium. q_m (mg/g) is the maximum adsorption capacity and K_L (L/mg) is the Langmuir constant, which are obtained from the slope and intercept of the plot for C_e/q_e vs. C_e , respectively. The value of R_L is the separation factor (a value between 0 and 1 indicates favorable adsorption, $R_L > 1$ represents unfavorable adsorption, $R_L = 1$ represents linear adsorption, and the procedure of adsorption is irre-

versible if $R_L = 0$). K_f and n are the two constants of the Freundlich isotherm and can be calculated from the intercept of the plot for $\ln q_e$ vs. $\ln C_e$.

As mentioned in Table 5, the Langmuir isotherm fit the experimental results better than the Freundlich isotherm for both compounds. The coefficient of correlations R^2 was very close to unity (0.98 and 0.99 for PCT and CPL, respectively). In addition, the maximum adsorption capacities calculated with this model for PCT and CPL were closer to those achieved experimentally. Based on the Langmuir isotherm, it was deduced that the surfaces of the ACs were covered with a monolayer of PCT or CPL molecules that did not interact with each other [43].

Table 5. Adsorption isotherm parameters.

	Langmuir Isotherm Parameters				Freundlich Isotherm Parameters		
	K_L (L/mg)	q_{max} (mg/g)	R_L	R^2	K_F (mg/g) (L/mg) ^{1/n}	1/n	R^2
PCT	3.53	71.42	0.007	0.98	31.14	0.48	0.90
CPL	1.20	166.66	0.020	0.99	143.65	0.128	0.98

3.2.7. Adsorption Thermodynamics

The determination of the evolution of the adsorption thermodynamics was crucial since they are essential to the process of adsorption. The thermodynamic variables of free energy (ΔG°), entropy variation (ΔS°) and enthalpy variation (ΔH°) demonstrate the feasibility and spontaneous character of adsorption. They help in comprehending the influence of temperature on the adsorption of PCT and CPL on the ACs surface [61]. The values for the thermodynamics parameters are presented in Table 6. These parameters are given by Equations (12) and (13) (Van 't Hoff equation) [57]:

$$\Delta G^\circ = -RT \ln K_d \quad (12)$$

$$\ln K_d = (\Delta S^\circ / R) - (\Delta H^\circ / RT) \quad (13)$$

where ΔG° is the standard free energy change, R is the universal gas constant (8.314, in J/mol.K), T is the absolute temperature (K), K_d is the equilibrium constant and ΔS° and ΔH° are the entropy and the enthalpy of the sorption reaction, respectively. These parameters were estimated from equilibrium uptake isotherms at the temperature range between 298 and 323 K.

Table 6. Thermodynamic adsorption parameters.

Adsorbate	ΔG° (KJ/mol)			ΔH° (KJ/mol)	ΔS° (J/mol.K)
	298 (K)	313 (K)	323 (K)		
PCT	−2.3	−3.5	−4.32	21.3	79.3
CPL	−5.0	−7.1	−8.5	34.9	138

As shown in Table 6, the endothermic adsorption was confirmed by the positive value of ΔH° for the PCT and CPL adsorption processes (21.3 and 34.9 KJ/mol for PCT and CPL, respectively). In addition, the physical origin of the adsorption process was confirmed by the values of ΔH° , which were below 40 KJ/mol. Therefore, the interactions between the PCT and CPL molecules and the ACs were ensured by electrostatic forces, such as dipole, van der Waals and hydrogen bonds [16,62]. Furthermore, the positive value of ΔS° indicated an increase in the disorder in the interaction between the ACs and the PCT and CPL molecules' surfaces during the adsorption process. The ΔS° of CPL is more important than the ΔS° of PCT. Thus, the affinity of CPL with the ACs was stronger than that of the PCT [63]. At the temperature range studied here, the uptake of PCT and CPL was favorable and spontaneous; this was indicated by the negative values of ΔG° . It is obvious that, as the temperature rose, the Gibbs free energy variation shrank, indicating that the adsorption

process became more significant. The increase in the temperature may have been caused by an expansion in the pores of the ACs, which helped bring about higher diffusion of PCT and CPL molecules into the ACs pores [64].

3.3. Experimental Design Performance

The above findings show that the dose of ACs and the initial concentration had impacts on the percentages of PCT and CPL removal, as did the pH for PCT removal. The RSM based on the CCD and BBD was applied to better understand the interactions between the parameters.

The responses achieved for the RSM model with the CCD and BBD were the removal percentages of PCT and CPL. The independent factors and their outcomes for this modelling are given in Tables 2 and 3. The developed ANOVA design is represented in Table 7. The analysis of the results collected confirmed that the model terms for PCT and CPL were significant because the *p*-values were lower than 0.05 (0.0013 for PCT and 0.0012 for CPL). The F-value was used to prioritize significant regression terms. The F-value was significant for the two models. It was equal to 24.25 for the PCT removal, with only a low probability of 0.13% that this value was due to noise. For the CPL, the F-value was also significant, with a value of 27.43 and only a 0.12% chance that it was due to the noise [32,65]. In addition, the regression term with the strongest F-value was recognized to be the most significant. The following are the rankings of good correlation factors for the two models based on F-values:

PCT model: $X_1 > X_2 > X_2^2 > X_2X_3 > X_3 > X_2^2 > X_1X_2 > X_1X_3$;

CPL model: $A_1 > A_2 > A_1^2 > A_2^2$.

Equations (14) and (15) provide semi-empirical expressions of the PCT and CPL removal, respectively, based on data analysis:

$$Y (\%) = 32.06708 + 0.154861 X_1 + 7.15264 X_2 - 0.997490 X_3 - 0.006637 X_1X_2 + 0.000356 X_1X_3 + 0.060111 X_2X_3 - 0.000060 X_2^2 - 0.72966 X_2^2 + 0.001078 X_3^2 \tag{14}$$

$$Y (\%) = 68.85360 + 0.155456 A_1 - 0.894490 A_2 + 0.001265 A_1A_2 - 0.000153 A_1^2 - 0.000838 A_2^2 \tag{15}$$

Table 7. ANOVA for both models (removal of PCT and CPL).

Model	Response	Sum of Squares	Degree of Freedom	Mean Square	F-Value	<i>p</i> -Value	R ²	R ² adj
PCT	Removal percentage	12,433.91	9	1381.55	24.25	0.0013	0.97	0.93
CPL	Removal percentage	10,361.16	5	2072.23	27.43	0.0012	0.96	0.92

Figure 6a,b show a comparison of the experimental values with the values predicted by the models for CPL and PCT removal, respectively. These graphics indicate that the models fit well. In addition, the coefficients of correlations (R² and adjusted R²_{adj}) for the two models shown in Table 7 were quite near unity, which confirmed the good relationship between the data [32]. The R² values were 0.97 and 0.96 for the PCT and CPL models, respectively. These results demonstrated the good robustness of the statistical models developed for both pharmaceutical removals. The resulting models' adaptability was confirmed by the adjusted R² (R²_{adj}) value, which was very close to the R² value for the two models (Table 7).

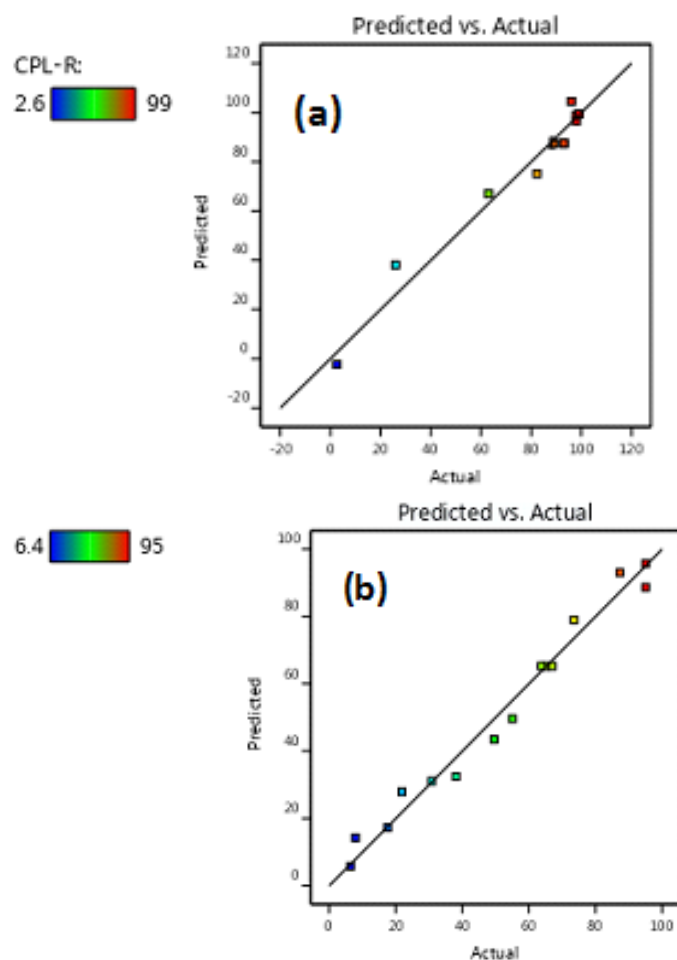


Figure 6. Actual vs. predicted values for the removal of CPL (a) and PCT (b).

The response functions developed with the multiple-factors model were used to predict the PCT and CPL removal. They were also used to reconstruct 3D surface plots, as presented in Figures 7 and 8, which show the response's behavior as a function of the interaction between two elements while keeping the third at the domain's center. Figure 7 demonstrates the effects of adsorbent dosage and CPL initial concentration on the removal percentages. It is clear that the dosage of ACs had a strong effect on the CPL removal. The increase in the ACs dose resulted in an important increase in the removal percentage for CPL. As shown in Figure 8, the results indicate that the percentage of PCT removal was more strongly affected by the ACs dose and the pH than the initial concentration of PCT.

The PCT and CPL removal rates determined under the optimum conditions ($C = 40$ mg/L, $\text{pH} = 7.5$ and ACs dosage = 750 mg/L for PCT and $C = 40$ mg/L and ACs dosage = 450 mg/L for CPL) were 85% and 98%, respectively. Under similar conditions, the PCT and CPL removal rates achieved with the models were 81% and 93.4% respectively. A slight difference between the two results was observed, which confirmed that the investigation of PCT and CPL adsorption could be optimized using an RSM based on the CCD and BBD models.

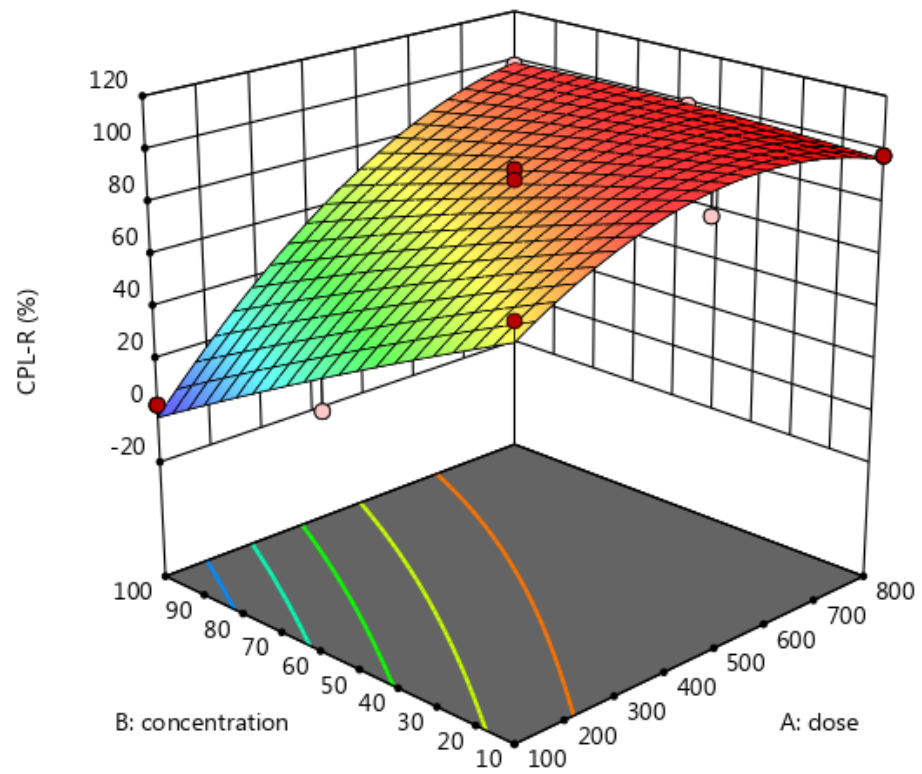


Figure 7. Response surface plot for the removal of CPL.

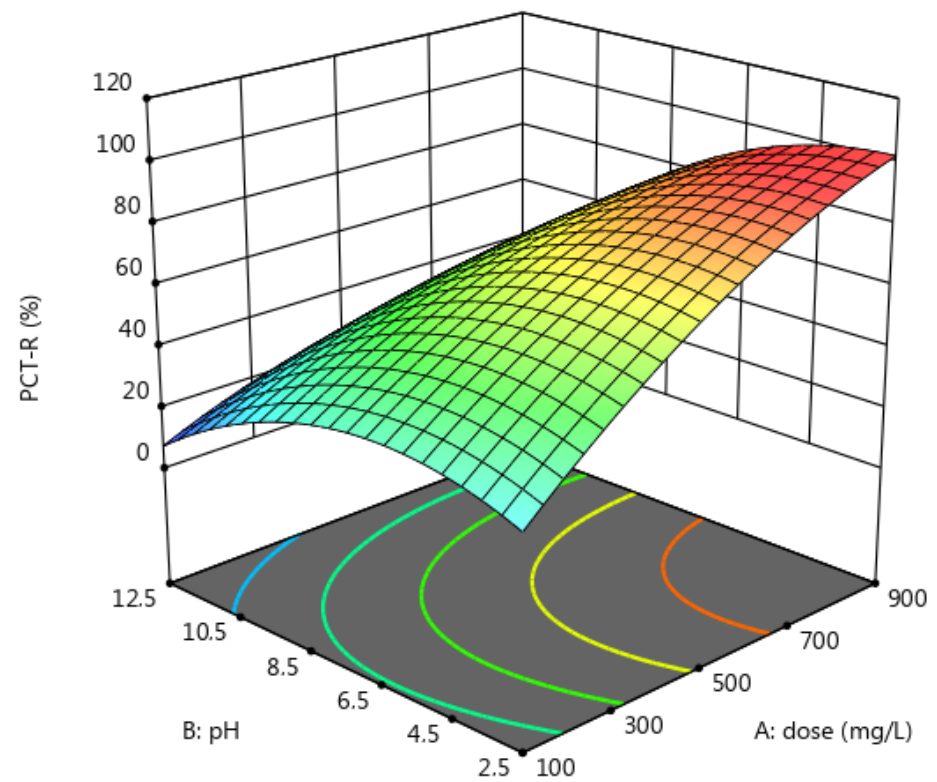


Figure 8. Cont.

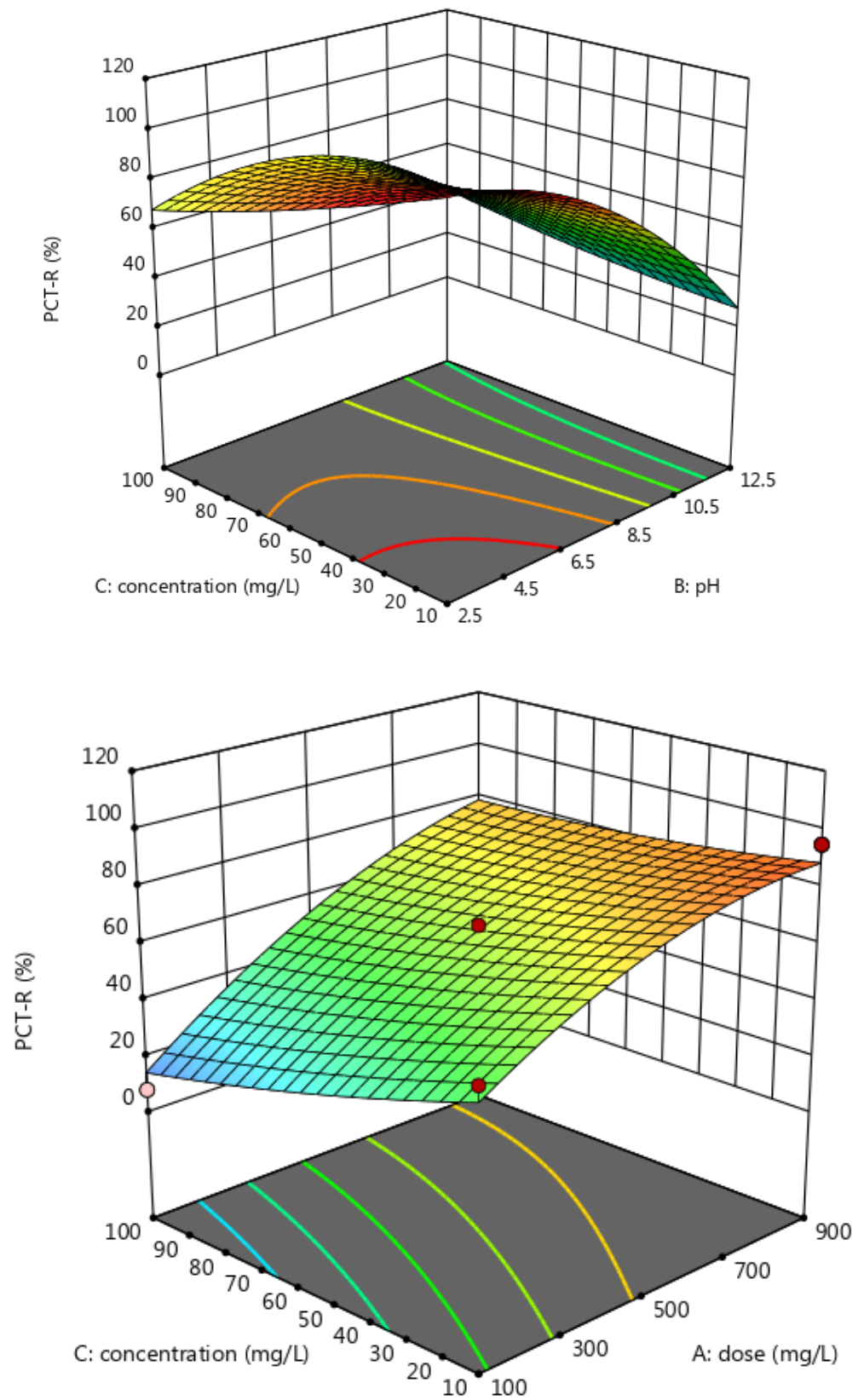


Figure 8. Response surface plots for the removal of PCT.

3.4. Comparison of the Performances of Different Activated Carbon Adsorbents

The performances of different kinds of activated carbon in PCT and CPL removal are summarized in Table 8. It is clear that the low-cost ACs had good performance compared to other kinds of low-cost activated carbon reported in the literature. In particular, the ACs prepared in this work presented high surface areas and maximum adsorption capacities under neutral pH for PCL and CPL compared to the results reported in the literature [43,48]. The maximum adsorption capacities were found at a pH of 7.5 (very close to neutrality). This was in contrast to many recent findings demonstrating that the best results were observed at low pH levels of 2, 3, 4, etc. [66–68], which require more effort to adjust the pH to a neutral range. The BET surface of the ACs in this study was greater than that reported by Li et al. [48], despite the similarity in the preparation method; the H₃PO₄/precursor weight ratio and the temperature of the pyrolysis were more important in this study, resulting in better synthesized ACs performances. Nguyen et al. and Kumar et al. [31–33] used sawdust to prepare activated carbon. They found good performances in terms of surface area (~1100 m²/g) and adsorption capacity but under acidic pH. It is also worth noting that it is difficult to undertake a real comparison when the treated substrates are different.

Table 8. Comparison of the performance of the low-cost activated carbon synthesized here with examples from the literature.

Adsorbent	BET (m ² /g)	Substrate	Findings	Retention (%)	Maximal Adsorption Capacity (mg/g)	Reference
Commercial activated carbon: F-300 F-100 WG-12 ROW 08 SUPRA Picabiol	860 730 1005 796 1344	Chloramphenicol	pH = 2 C = 161 mg/L T = 20 °C Dose: 4000 mg/L t = 480 min t = 600 min t = 600 min t = 600 min t = 360 min	-	200 174 195 212 214	[19]
Acid-treated beverage sludge-activated carbon (ABSAC)	642	Paracetamol	pH = 8 C = 50 mg/L t = 30 min T = 25 °C Dose: 800 mg/L	86	145.4	[21]
AC based on sawdust	1695	Rhodamine B	pH = 3 C = 10mg/L t = 10 min T = 25 °C Dose: 1000 mg/L	100	300	[31]
AC based on sawdust	1409	Naphthalene	pH = 2 C = 30 mg/L t = 90 min T = 25 °C Dose: 333 mg/L	96	-	[33]
AC from endocarp of the species <i>Butia capitata</i>	820	Paracetamol	pH = 8 C = 50 mg/L t = 180 min T = 25 °C Dose: 1000 mg/L	81	100	[43]
AC from oak acorns	234	Paracetamol	pH = 3 t = 150 min T = 25 °C Dose: 100 mg/L	-	45	[45]
Activated carbon based on corn stover	961	Chloramphenicol	pH = 7 C = 25 mg/L t = 120 min T = 25 °C Dose: 8000 mg/L	100	32.3	[46]

Table 8. Cont.

Adsorbent	BET (m ² /g)	Substrate	Findings	Retention (%)	Maximal Adsorption Capacity (mg/g)	Reference
Activated carbon based on <i>Typha orientalis</i>	794.8	Chloramphenicol	pH = 6.2 C = 65 mg/L t = 360 min T = 25 °C Dose: 600 mg/L	87	137	[48]
Bamboo charcoal-based biochar	<1	Chloramphenicol	C = 20 mg/L t = 15 min T = 25 °C Dose: 8000 mg/L	-	0.65	[61]
Sodium hydroxide-modified bamboo charcoal	<1	Chloramphenicol	C = 20 mg/L t = 15 min T = 25 °C Dose: 8000 mg/L	-	2.35	[69]
Biochars pyrolyzed at 350 °C	-	Chloramphenicol	pH = 7 C = 40 mg/L t = 1080 min T = 25 °C Dose: 500 mg/L	-	10	[66]
Biochars pyrolyzed at 500 °C	-	Chloramphenicol	pH = 7 C = 40 mg/L t = 1080 min T = 25 °C Dose: 500 mg/L	-	14.2	[66]
Biochars pyrolyzed at 700 °C	-	Chloramphenicol	pH = 7 C = 40 mg/L t = 1080 min T = 25 °C Dose: 500 mg/L	-	33	[66]
H ₃ PO ₄ -activated biochar at 600 °C	-	Chloramphenicol	pH = 4 C = 20 mg/L t = 1800 min T = 25 °C Dose: 80 mg/L	-	21	[67]
AC from babassu coconut	484	Paracetamol	pH = 3.9 C = 25 mg/L t > 200 min T = 25 °C Dose: 3.5–3000 mg/L	-	71	[68]
AC from dende coconut	672	Paracetamol	pH = 6.5 C = 25 mg/L t > 90 min T = 25 °C Dose: 3.5–3000 mg/L	-	70	[68]
Two activated carbons: CAT CARBOPAL	983 1588	Paracetamol	pH = 3 C = 150 mg/L t = 800 min T = 25 °C Dose: 167 mg/L	-	560 450	[70]
AC based on sawdust	303–1298	Chloramphenicol	pH = 7.5 C = 40 mg/L t = 90 min T = 25 °C Dose: 450 mg/L	98	176	This work
AC from sawdust	303–1298	Paracetamol	pH = 7.5 C = 40 mg/L t = 20 min T = 25 °C Dose: 750 mg/L	85	92	This work

The prepared ACs exhibited excellent adsorption efficiency for pharmaceutical compounds compared to the examples from the literature.

4. Conclusions

Low-cost activated carbon (ACs) was successfully prepared from sawdust using the chemical method with H_3PO_4 and showed remarkable properties. This study demonstrated that the ACs could be used efficiently for the removal of PCT and CPL from real wastewater. The results showed that the adsorption rates in the removal of both pharmaceuticals were very rapid, and this was due to the physical interactions between the PCT and the ACs and the CPL and the ACs. The pseudo-second-order kinetic model and the Langmuir isotherm model showed the best statistical adjustments for the uptake of the PCT and CPL, with maximum adsorption capacities of 92 mg/g and 176 mg/g, respectively. The thermodynamics study led us to conclude that an endothermic process occurred for both pharmaceutical compounds (ΔH° of PCT = 21.3 KJ/mol; ΔH° of CPL = 34.9 KJ/mol).

The removal of PCT and CPL was successfully optimized using an RSM based on the CCD and BBD. Following the evaluation and selection of models using statistical analysis, ANOVA was used to examine the various parameters. The influences of various factors, including ACs dose, initial concentration and pH, were determined. For the removal of both substances, it was observed that the dosage of ACs was the most important factor.

These findings allow us to conclude that sawdust is a suitable raw material for successfully developing activated carbon with potential applications relating to the removal of pharmaceuticals from wastewater.

Author Contributions: Conceptualization, C.C. and R.B.A.; Data curation, M.R.; Investigation, M.R., A.A. (Afef Attia), C.C., S.M.-C., A.A. (Ayten Ates), J.D. and R.B.A.; Methodology, M.R.; Project administration, R.B.A.; Software, M.R., A.A. (Afef Attia), A.A. (Ayten Ates) and J.D.; Supervision, C.C. and R.B.A.; Validation, C.C., S.M.-C. and R.B.A.; Writing—original draft, M.R. and C.C.; Writing—review and editing, S.M.-C. and R.B.A. All authors have read and agreed to the published version of the manuscript.

Funding: The paper is supported by the PRIMA 2020 program under agreement No°2024–TRUST project (The PRIMA program is supported by the European Union) and PHC-Utique project 20G1205.

Institutional Review Board Statement: Not applicable.

Informed Consent Statement: Not applicable.

Data Availability Statement: The data presented in this study are available on request from the corresponding author.

Acknowledgments: The authors gratefully acknowledge funding from TRUST Prima program (research project supported by the European commission).

Conflicts of Interest: The authors declare no conflict of interest.

References

1. Imanipoor, J.; Mohammadi, M.; Dinari, M. Evaluating the performance of L-methionine modified montmorillonite K10 and 3-aminopropyltriethoxysilane functionalized magnesium phyllosilicate organoclays for adsorptive removal of azithromycin from water. *Sep. Purif. Technol.* **2021**, *275*, 119256. [[CrossRef](#)]
2. Geissen, V.; Mol, H.; Klumpp, E.; Umlauf, G.; Nadal, M.; Van der Ploeg, M.; Ritsema, C.J. Emerging pollutants in the environment: A challenge for water resource management. *Int. Soil Water Conserv. Res.* **2015**, *3*, 57–65. [[CrossRef](#)]
3. El Bekkali, C.; Bouyarmane, H.; El Karbane, M.; Masse, S.; Saoiabi, A.; Coradin, T.; Laghizil, A. Zinc oxide-hydroxyapatite nanocomposite photocatalysts for the degradation of ciprofloxacin and ofloxacin antibiotics. *Colloids Surf. A Physicochem. Eng. Asp.* **2018**, *539*, 364–370. [[CrossRef](#)]
4. Dahane, S.; García, M.G.; Bueno, M.M.; Moreno, A.U.; Galera, M.M.; Derdour, A. Determination of drugs in river and wastewaters using solid-phase extraction by packed multi-walled carbon nanotubes and liquid chromatography-quadrupole-linear ion trap-mass spectrometry. *J. Chromatogr. A.* **2013**, *1297*, 17–28. [[CrossRef](#)]
5. Peña-Guzmán, C.; Ulloa-Sánchez, S.; Mora, K.; Helena-Bustos, R.; Lopez-Barrera, E.; Alvarez, J.; Rodriguez-Pinzón, M. Emerging pollutants in the urban water cycle in Latin America: A review of the current literature. *J. Environ. Manag.* **2019**, *237*, 408–423. [[CrossRef](#)] [[PubMed](#)]

6. Montes-Grajales, D.; Fennix-Agudelo, M.; Miranda-Castro, W. Occurrence of personal care products as emerging chemicals of concern in water resources: A review. *Sci. Total Environ.* **2017**, *595*, 601–614. [[CrossRef](#)]
7. Ghosh, G.; Hanamoto, S.; Yamashita, N.; Huang, X.; Tanaka, H. Antibiotics removal in biological sewage treatment plants. *Pollution* **2016**, *2*, 131–139.
8. Xu, L.; Zhang, H.; Xiong, P.; Zhu, Q.; Liao, C.; Jiang, G. Occurrence, fate, and risk assessment of typical tetracycline antibiotics in the aquatic environment: A review. *Sci. Total Environ.* **2021**, *753*, 141975. [[CrossRef](#)]
9. Gu, X.; Xu, Z.; Gu, L.; Xu, H.; Han, F.; Chen, B.; Pan, X. Preparation and antibacterial properties of gold nanoparticles: A review. *Environ. Chem. Lett.* **2021**, *19*, 167–187. [[CrossRef](#)]
10. Zhang, T.; Yang, Y.; Li, X.; Jiang, Y.; Fan, X.; Du, P.; Zhou, Z. Adsorption characteristics of chloramphenicol onto powdered activated carbon and its desorption performance by ultrasound. *Environ. Technol.* **2021**, *42*, 571–583. [[CrossRef](#)]
11. Nguyen, L.M.; Nguyen, N.T.T.; Nguyen, T.T.T.; Nguyen, T.T.; Nguyen, D.T.C.; Tran, T.V. Occurrence, toxicity and adsorptive removal of the chloramphenicol antibiotic in water: A review. *Environ. Chem. Lett.* **2022**, *20*, 1929–1963. [[CrossRef](#)]
12. Tran, H.N.; Tomul, F.; Ha, N.T.H.; Nguyen, D.T.; Lima, E.C.; Le, G.T.; Woo, S.H. Innovative spherical biochar for pharmaceutical removal from water: Insight into adsorption mechanism. *J. Hazard. Mater.* **2020**, *394*, 122255. [[CrossRef](#)] [[PubMed](#)]
13. Damasceno de Oliveira, L.L.; Nunes, B.; Antunes, S.C.; Campitelli-Ramos, R.; Rocha, O. Acute and chronic effects of three pharmaceutical drugs on the tropical freshwater cladoceran *Ceriodaphnia silvestrii*. *Water Air Soil Pollut.* **2018**, *4*, 116. [[CrossRef](#)]
14. Żur, J.; Wojcieszynska, D.; Hupert-Kocurek, K.; Marchlewicz, A.; Guzik, U. Paracetamol–toxicity and microbial utilization. *Pseudomonas moorei* KB4 as a case study for exploring degradation pathway. *Chemosphere* **2018**, *206*, 192–202. [[CrossRef](#)] [[PubMed](#)]
15. Kujawska, A.; Kielkowska, U.; Atisha, A.; Yanful, E.; Kujawski, W. Comparative analysis of separation methods used for the elimination of pharmaceuticals and personal care products (PPCPs) from water—A critical review. *Sep. Purif. Technol.* **2022**, *290*, 120797. [[CrossRef](#)]
16. Romdhani, M.; Aloulou, W.; Aloulou, H.; Charcosset, C.; Mahouche-Chergui, S.; Carbonnier, B.; Ben Amar, R. Performance studies of indigo dye removal using TiO₂ modified clay and zeolite ultrafiltration membrane hybrid system. *Desalin. Water Treat.* **2021**, *243*, 262–274. [[CrossRef](#)]
17. Yousefi, M.; Arami, S.M.; Takallo, H.; Hosseini, M.; Radfard, M.; Soleimani, H.; Mohammadi, A.A. Modification of pumice with HCl and NaOH enhancing its fluoride adsorption capacity: Kinetic and isotherm studies. *Hum. Ecol. Risk Assess. HERA* **2018**, *25*, 1508–1520. [[CrossRef](#)]
18. Gopinath, A.; Kadirvelu, K. Strategies to design modified activated carbon fibers for the decontamination of water and air. *Environ. Chem. Lett.* **2018**, *16*, 1137–1168. [[CrossRef](#)]
19. Lach, J. Adsorption of chloramphenicol on commercial and modified activated carbons. *Water* **2019**, *11*, 1141. [[CrossRef](#)]
20. Abdulsalam, K.A.; Giwa, A.R.A.; Adelowo, J.M. Optimization studies for decolourization of textile wastewater using a sawdust-based adsorbent. *Chem. Data Collect.* **2020**, *27*, 100400. [[CrossRef](#)]
21. Streit, A.F.; Collazzo, G.C.; Druzian, S.P.; Verdi, R.S.; Foletto, E.L.; Oliveira, L.F.; Dotto, G.L. Adsorption of ibuprofen, ketoprofen, and paracetamol onto activated carbon prepared from effluent treatment plant sludge of the beverage industry. *Chemosphere* **2021**, *262*, 128322. [[CrossRef](#)] [[PubMed](#)]
22. Heidarinejad, Z.; Dehghani, M.H.; Heidari, M.; Javedan, G.; Ali, I.; Sillanpää, M. Methods for preparation and activation of activated carbon: A review. *Environ. Chem. Lett.* **2020**, *18*, 393–415. [[CrossRef](#)]
23. Bouchelta, C.; Medjram, M.S.; Bertrand, O.; Bellat, J.P. Preparation and characterization of activated carbon from date stones by physical activation with steam. *J. Anal. Appl. Pyrolysis* **2008**, *82*, 70–77. [[CrossRef](#)]
24. Yahya, M.A.; Al-Qodah, Z.; Ngah, C.Z. Agricultural bio-waste materials as potential sustainable precursors used for activated carbon production: A review. *Renew. Sustain. Energy Rev.* **2015**, *46*, 218–235. [[CrossRef](#)]
25. Yorgun, S.; Yıldız, D. Preparation and characterization of activated carbons from Paulownia wood by chemical activation with H₃PO₄. *Taiwan Inst. Chem. Eng.* **2015**, *53*, 122–131. [[CrossRef](#)]
26. Abbasi, S.; Mirghorayshi, M.; Zinadini, S.; Zinatizadeh, A.A. A novel single continuous electrocoagulation process for treatment of licorice processing wastewater: Optimization of operating factors using RSM. *Process Saf. Environ. Prot.* **2020**, *134*, 323–332. [[CrossRef](#)]
27. Abdullah, N.; Saidur, R.; Zainoodin, A.M.; Aslfattahi, N. Optimization of electrocatalyst performance of platinum–ruthenium induced with MXene by response surface methodology for clean energy application. *J. Clean. Prod.* **2020**, *277*, 123395. [[CrossRef](#)]
28. Bheemanapally, K.; Ibrahim, M.M.; Briski, K.P. Optimization of ultra-high-performance liquid chromatography-electrospray ionization-mass spectrometry detection of glutamine-FMOC ad-hoc derivative by central composite design. *Sci. Rep.* **2020**, *10*, 7134. [[CrossRef](#)]
29. Sakkas, V.A.; Islam, M.A.; Stalikas, C.; Albanis, T.A. Photocatalytic degradation using design of experiments: A review and example of the Congo red degradation. *J. Hazard. Mater.* **2010**, *175*, 33–44. [[CrossRef](#)]
30. Oladimeji, T.E.; Odunoye, B.O.; Elehinafe, F.B.; Oyinlola, R.O.; Olayemi, A.O. Production of activated carbon from sawdust and its efficiency in the treatment of sewage water. *Heliyon* **2021**, *7*, e05960. [[CrossRef](#)]
31. Nguyen, D.T.; Nguyen, T.T.; Nguyen, H.P.T.; Khuat, H.B.; Nguyen, T.H.; Tran, V.K.; La, D.D. Activated carbon with ultrahigh surface area derived from sawdust biowaste for the removal of rhodamine B in water. *Environ. Technol. Innov.* **2021**, *24*, 101811. [[CrossRef](#)]

32. Belgada, A.; Charik, F.Z.; Achiou, B.; Kambuyi, T.N.; Younssi, S.A.; Beniazza, R.; Ouammou, M. Optimization of phosphate/kaolinite microfiltration membrane using Box–Behnken design for treatment of industrial wastewater. *J. Environ. Chem. Eng.* **2021**, *9*, 104972. [[CrossRef](#)]
33. Kumar, A.; Gupta, H. Activated carbon from sawdust for naphthalene removal from contaminated water. *Environ. Technol. Innov.* **2020**, *20*, 101080. [[CrossRef](#)]
34. Gupta, H.; Gupta, B. Adsorption of polycyclic aromatic hydrocarbons on banana peel activated carbon. *Desalin. Water Treat.* **2016**, *57*, 9498–9509. [[CrossRef](#)]
35. Puchana-Rosero, M.J.; Adebayo, M.A.; Lima, E.C.; Machado, F.M.; Thue, P.S.; Vaggetti, J.C.; Gutterres, M. Microwave-assisted activated carbon obtained from the sludge of tannery-treatment effluent plant for removal of leather dyes. *Colloids Surf. A Physicochem. Eng. Asp.* **2016**, *504*, 105–115. [[CrossRef](#)]
36. Xu, F.; Yu, J.; Tesso, T.; Dowell, F.; Wang, D. Qualitative and quantitative analysis of lignocellulosic biomass using infrared techniques: A mini-review. *Appl. Energy* **2013**, *104*, 801–809. [[CrossRef](#)]
37. Lima, D.R.; Hosseini-Bandegharai, A.; Thue, P.S.; Lima, E.C.; de Albuquerque, Y.R.; dos Reis, G.S.; Tran, H.N. Efficient acetaminophen removal from water and hospital effluents treatment by activated carbons derived from Brazil nutshells. *Colloids Surf. A Physicochem. Eng. Asp.* **2019**, *583*, 123966. [[CrossRef](#)]
38. Hamed, M.M.; Ali, M.M.S.; Holiel, M. Preparation of activated carbon from doum stone and its application on adsorption of ^{60}Co and $^{152+154}\text{Eu}$: Equilibrium, kinetic and thermodynamic studies. *J. Environ. Radioact.* **2016**, *164*, 113–124. [[CrossRef](#)]
39. Baccar, R.; Bouzid, J.; Feki, M.; Montiel, A. Preparation of activated carbon from Tunisian olive-waste cakes and its application for adsorption of heavy metal ions. *J. Hazard. Mater.* **2009**, *162*, 1522–1529. [[CrossRef](#)]
40. Jiang, G.; Qiao, J.; Hong, F. Application of phosphoric acid and phytic acid-doped bacterial cellulose as novel proton-conducting membranes to PEMFC. *Int. J. Hydrog. Energy* **2012**, *37*, 9182–9192. [[CrossRef](#)]
41. Jedynak, K.; Szczepanik, B.; Rędzia, N.; Słomkiewicz, P.; Kolbus, A.; Rogala, P. Ordered mesoporous carbons for adsorption of paracetamol and non-steroidal anti-inflammatory drugs: Ibuprofen and naproxen from aqueous solutions. *Water* **2019**, *11*, 1099. [[CrossRef](#)]
42. Sing, K.S. Reporting physisorption data for gas/solid systems with special reference to the determination of surface area and porosity (Recommendations 1984). *Pure Appl. Chem.* **1985**, *57*, 603–619. [[CrossRef](#)]
43. Kerkhoff, C.M.; da Boit Martinello, K.; Franco, D.S.; Netto, M.S.; Georgin, J.; Foletto, E.L.; Dotto, G.L. Adsorption of ketoprofen and paracetamol and treatment of a synthetic mixture by novel porous carbon derived from *Butia capitata* endocarp. *J. Mol. Liq.* **2021**, *339*, 117184. [[CrossRef](#)]
44. Patania, F.; Gagliano, A.; Nocera, F.; Galesi, A. The pollution of water resources and interventions to mitigate and control environmental impact. *Water Soc.* **2012**, *153*, 299.
45. Nourmoradi, H.; Moghadam, K.F.; Jafari, A.; Kamarehie, B. Removal of acetaminophen and ibuprofen from aqueous solutions by activated carbon derived from *Quercus Brantii* (Oak) acorn as a low-cost biosorbent. *J. Environ. Chem. Eng.* **2018**, *6*, 6807–6815. [[CrossRef](#)]
46. Cheng, X.; Zheng, C.; Lu, Q.; Liu, J.; Wang, Q.; Fan, Y.; Zhang, J. Adsorption of furazolidone, D-cycloserine, and chloramphenicol on granular activated carbon made from corn stover. *J. Environ. Chem. Eng.* **2019**, *145*, 04019038. [[CrossRef](#)]
47. Mashayekh-Salehi, A.; Moussavi, G. Removal of acetaminophen from the contaminated water using adsorption onto carbon activated with NH_4Cl . *Desalin. Water Treat.* **2016**, *57*, 12861–12873. [[CrossRef](#)]
48. Li, Y.; Zhang, J.; Liu, H. Removal of chloramphenicol from aqueous solution using low-cost activated carbon prepared from *Typha orientalis*. *Water* **2018**, *10*, 351. [[CrossRef](#)]
49. Zhu, X.; Gao, Y.; Yue, Q.; Song, Y.; Gao, B.; Xu, X. Facile synthesis of hierarchical porous carbon material by potassium tartrate activation for chloramphenicol removal. *J. Taiwan Inst. Chem. Eng.* **2018**, *85*, 141–148. [[CrossRef](#)]
50. Zhang, R.; Zhou, Z.; Xie, A.; Dai, J.; Cui, J.; Lang, J.; Yan, Y. Preparation of hierarchical porous carbons from sodium carboxymethyl cellulose via halloysite template strategy coupled with KOH-activation for efficient removal of chloramphenicol. *J. Taiwan Inst. Chem. Eng.* **2017**, *80*, 424–433. [[CrossRef](#)]
51. Zhao, X.; Zhao, H.; Dai, W.; Wei, Y.; Wang, Y.; Zhang, Y.; Gao, Z. A metal-organic framework with large 1-D channels and rich OH sites for high-efficiency chloramphenicol removal from water. *J. Colloid Interface Sci.* **2018**, *526*, 28–34. [[CrossRef](#)] [[PubMed](#)]
52. Pauletto, P.S.; Lütke, S.F.; Dotto, G.L.; Salau, N.P.G. Forecasting the multicomponent adsorption of nimesulide and paracetamol through artificial neural network. *Chem. Eng. J.* **2021**, *412*, 127527. [[CrossRef](#)]
53. Lim, S.; Kim, J.H.; Park, H.; Kwak, C.; Yang, J.; Kim, J.; Lee, J. Role of electrostatic interactions in the adsorption of dye molecules by $\text{Ti}_3\text{C}_2\text{-MXenes}$. *RSC Adv.* **2021**, *11*, 6201–6211. [[CrossRef](#)] [[PubMed](#)]
54. Chitongo, R.; Opeolu, B.O.; Olatunji, O.S. Abatement of amoxicillin, ampicillin, and chloramphenicol from aqueous solutions using activated carbon prepared from grape slurry. *CLEAN—Soil Air Water* **2019**, *47*, 1800077. [[CrossRef](#)]
55. Idris, Z.M.; Hameed, B.H.; Ye, L.; Hajizadeh, S.; Mattiasson, B.; Din, A.M. Amino-functionalised silica-grafted molecularly imprinted polymers for chloramphenicol adsorption. *J. Environ. Chem. Eng.* **2020**, *8*, 103981. [[CrossRef](#)]
56. Cizmas, L.; Sharma, V.K.; Gray, C.M.; McDonald, T.J. Pharmaceuticals and personal care products in waters: Occurrence, toxicity, and risk. *Environ. Chem. Lett.* **2015**, *13*, 381–394. [[CrossRef](#)]

57. Kuśmierk, K.; Świątkowski, A.; Kotkowski, T.; Cherbański, R.; Molga, E. Adsorption on activated carbons from end-of-life tyre pyrolysis for environmental applications. Part II. Adsorption from aqueous phase. *J. Anal. Appl. Pyrolysis* **2021**, *158*, 105206. [[CrossRef](#)]
58. Noorimotlagh, Z.; Soltani, R.D.C.; Khataee, A.R.; Shahriyar, S.; Nourmoradi, H. Adsorption of a textile dye in aqueous phase using mesoporous activated carbon prepared from Iranian milk vetch. *J. Taiwan Inst. Chem. Eng.* **2014**, *45*, 1783–1791. [[CrossRef](#)]
59. Langmuir, I. The adsorption of gases on plane surfaces of glass, mica and platinum. *J. Am. Chem. Soc.* **1918**, *40*, 1361–1403. [[CrossRef](#)]
60. Freundlich, H.M.F. Over the Adsorption in Solution. *J. Phys. Chem.* **1906**, *57*, 385–471.
61. Balarak, D.; Zafariyan, M.; Igwegbe, C.A.; Onyechi, K.K.; Ighalo, J.O. Adsorption of acid blue 92 dye from aqueous solutions by single-walled carbon nanotubes: Isothermal, kinetic, and thermodynamic studies. *Environ. Process.* **2021**, *8*, 869–888. [[CrossRef](#)]
62. Dutta, M.; Das, U.; Mondal, S.; Bhattacharya, S.; Khatun, R.; Bagal, R. Adsorption of acetaminophen by using tea waste derived activated carbon. *Int. J. Environ. Sci.* **2015**, *6*, 270. [[CrossRef](#)]
63. Zanella, O.; Klein, É.; Haro, N.K.; Cardoso, M.G.; Tessaro, I.C.; Féris, L.A. Equilibrium studies, kinetics and thermodynamics of anion removal by adsorption. *World Rev. Sci. Technol. Sustain. Dev.* **2016**, *12*, 193–218. [[CrossRef](#)]
64. Pei, Y.; Agostini, F.; Skoczylas, F. The effects of high temperature heating on the gas permeability and porosity of a cementitious material. *Cem. Concr. Res.* **2017**, *95*, 141–151. [[CrossRef](#)]
65. Addar, F.Z.; El-Ghizizel, S.; Tahaikt, M.; Belfaquir, M.; Taky, M.; Elmidaoui, A. Fluoride removal by nanofiltration: Experimentation, modelling and prediction based on the surface response method. *Desalin. Water Treat.* **2021**, *240*, 75–88. [[CrossRef](#)]
66. Yang, F.; Zhang, Q.; Jian, H.; Wang, C.; Xing, B.; Sun, H.; Hao, Y. Effect of biochar-derived dissolved organic matter on adsorption of sulfamethoxazole and chloramphenicol. *J. Hazard. Mater.* **2020**, *396*, 122598. [[CrossRef](#)]
67. Ahmed, M.B.; Zhou, J.L.; Ngo, H.H.; Guo, W.; Johir, M.A.H.; Belhaj, D. Competitive sorption affinity of sulfonamides and chloramphenicol antibiotics toward functionalized biochar for water and wastewater treatment. *Bioresour. Technol.* **2017**, *238*, 306–312. [[CrossRef](#)]
68. Ferreira, R.C.; De Lima, H.H.C.; Cândido, A.A.; Junior, O.C.; Arroyo, P.A.; De Carvalho, K.Q.; Barros, M.A.S.D. Adsorption of paracetamol using activated carbon of dende and babassu coconut mesocarp. *Int. J. Biotechnol. Bioeng.* **2015**, *9*, 717–722.
69. Fan, Y.; Wang, B.; Yuan, S.; Wu, X.; Chen, J.; Wang, L. Adsorptive removal of chloramphenicol from wastewater by NaOH modified bamboo charcoal. *Bioresour. Technol.* **2010**, *101*, 7661–7664. [[CrossRef](#)]
70. Spaltro, A.; Pila, M.N.; Colasurdo, D.D.; Grau, E.N.; Román, G.; Simonetti, S.; Ruiz, D.L. Removal of paracetamol from aqueous solution by activated carbon and silica. Experimental and computational study. *J. Contam. Hydrol.* **2021**, *236*, 103739. [[CrossRef](#)]

Disclaimer/Publisher’s Note: The statements, opinions and data contained in all publications are solely those of the individual author(s) and contributor(s) and not of MDPI and/or the editor(s). MDPI and/or the editor(s) disclaim responsibility for any injury to people or property resulting from any ideas, methods, instructions or products referred to in the content.